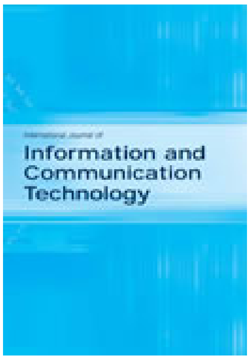

International Journal of Information and Communication Technology

ISSN online: 1741-8070 - ISSN print: 1466-6642
https://www.inderscience.com/ijict

Energy supply chain financial risk prediction based on GNN and multi-source time series data

Pei Wan, Juanjuan Jiang

DOI: 10.1504/IJICT.2026.10075489

Article History:

Received:	12 September 2025
Last revised:	16 October 2025
Accepted:	19 October 2025
Published online:	22 January 2026

Energy supply chain financial risk prediction based on GNN and multi-source time series data

Pei Wan and Juanjuan Jiang*

School of Management,
Guangzhou City University of Technology,
Guangdong, 510800, China
Email: wanpei@gcu.edu.cn
Email: JuanjuanJiangg@outlook.com
*Corresponding author

Abstract: The energy industry is characterised by strong cyclicality, network infection risk, and multi-source data heterogeneity, making it difficult for traditional static assessment models of supply chain finance to meet dynamic early warning needs. To address these challenges, this paper proposes a dynamic heterogeneous graph neural network (DHGNN) model, which integrates a dynamic graph structure with cross-modal fusion of multi-source time series data, including finance, logistics, and public opinion. The core innovations of the model include a spatiotemporal attention mechanism, a dynamic graph construction module, and an industry-specific indicator system. Verification on the energy industry dataset demonstrates that the early warning accuracy reaches 96.2% (F1 = 0.974, AUC (area under the ROC curve) = 0.962), with an average early warning time of 6.8 months ahead of schedule, which is 40% higher than existing models, and the risk transmission path identification accuracy increased by 32%.

Keywords: graph neural network; GNN; multimodal time series fusion; risk dynamic prediction; energy supply chain finance.

Reference to this paper should be made as follows: Wan, P. and Jiang, J. (2026) 'Energy supply chain financial risk prediction based on GNN and multi-source time series data', *Int. J. Information and Communication Technology*, Vol. 27, No. 1, pp.60–76.

Biographical notes: Pei Wan is a faculty member at Guangzhou City University of Technology. Her research spans financial technology, corporate finance, and supply chain finance. Her research examines financial decision-making and risk exposure in corporate and supply chain finance, with particular focus on how digital transformation shapes financial strategies.

Juanjuan Jiang is a faculty member at Guangzhou City University of Technology. Her research spans financial technology, corporate finance, and supply chain finance. Her work focuses on corporate risk management, developing systematic frameworks for risk identification and assessment to support organisational risk mitigation.

1 Introduction

The supply chain finance of energy companies is facing severe triple challenges. First, the risk is extremely dynamic and vulnerable to the impact of many factors. On the one hand, commodity prices are constantly fluctuating; on the other hand, policy regulations such as the 'double carbon' policy are constantly advancing, coupled with the invasion of natural disasters; these factors make the risk extremely unstable, which may have an impact on supply chain finance at any time (Gu et al., 2023). Secondly, the network contagion effect is prominent. The supply chain is not an isolated collection of individuals but a closely connected whole. Once the core enterprise has credit risk, this risk will spread quickly in the supply chain like ripples. Judging from past cases, due to supplier default, the risk of a central enterprise was transmitted along the supply chain, which eventually led to the indirect break of its capital chain. This also fully exposed that the traditional single-point assessment model has failed when dealing with the financial risks of complex supply chains, and it is impossible to control the whole picture of risks (Hu et al., 2024) accurately. Third, the data presents a complex state of multi-source heterogeneity. The ERP system within the enterprise carries detailed financial time series data, and a large amount of GPS trajectory data is generated in logistics and transportation links (Chen et al., 2025). In addition, public opinion text data is also generated at all times. Due to diverse sources and different structures, these multi-modal data have not been effectively integrated for a long time, resulting in numerous information islands, which cannot provide comprehensive and accurate data support for risk assessment and decision-making of supply chain finance, which seriously restricts the efficient development and stable operation of supply chain finance for energy enterprises (Wojewska et al., 2024).

The existing methods have obvious limitations in risk management, which are mainly reflected in the following three aspects: First, the BP neural network model relies too much on the single data source of enterprise financial statements but completely ignores real-time operating data (such as sales orders, inventory turnover, capital flow, etc.), resulting in lag risk perception and difficulty in capturing dynamic risk changes (Qiu and Gao, 2025); secondly, the traditional risk control framework does not model and analyse complex enterprise relationships, such as guarantee network, capital exchange, counterparty map, etc. A large bank once suffered a loss of more than 10 million Yuan in supply chain financing because it failed to identify the hidden fraud of affiliated enterprise clusters (Gou et al., 2025). Third, multi-source time series data (such as equipment operating rate, logistics, transportation index, public opinion popularity, etc.) and supply chain topology have not been effectively integrated (Li et al., 2024), resulting in the data separation of time series dimension and relationship dimension, and a complete risk portrait cannot be formed. For example, separate enterprise import and export data analysis cannot reveal key node risks in the supply chain when monitoring trade financing risks. In contrast, the lack of map analysis of upstream and downstream enterprise transaction relationships may lead to misjudgment of systemic risks (Wang et al., 2023).

Under this background, this paper has made three innovative achievements in the field of risk prediction in the energy industry: First, a unified framework based on dynamic heterogeneous graph neural network (DHGNN) is proposed (Ouyang et al., 2025), which for the first time deeply integrates the construction of dynamic transaction relationships of enterprises with the extraction of multi-source time series features (such as equipment operating rate and logistics index), breaking the traditional fragmented mode of ‘static diagrams + independent timing’ (Sang et al., 2025). Secondly, a cross-modal feature fusion module is designed to effectively integrate structured financial data, unstructured text information, and sensor time series data in the energy field through a multi-level attention mechanism, solving the industry’s long-standing problem of data heterogeneity. Finally, a specific risk indicator system for the energy industry covering seven dimensions – including policy sensitivity, environmental compliance risks, and supply chain stability – is built to provide the model with an assessment basis that aligns more closely with industry characteristics and significantly improves the accuracy and forward-lookingness of risk identification.

In the context of supply chain finance, especially within the energy industry, several critical questions arise regarding the effective management and early warning of financial risks. Firstly, how can we simultaneously capture the temporal evolution and topological contagion of supply chain financial risk? This is crucial given the dynamic nature of financial risks and their potential to propagate through complex network structures. Secondly, how can we effectively fuse heterogeneous modal data, which often have inconsistent sampling rates and distributions? This challenge is particularly pertinent in the energy sector, where data sources such as financial records, logistics information, and public opinion vary significantly in their characteristics. Lastly, how can we ensure the model’s interpretability and early-warning lead time in real-world energy finance scenarios? Addressing these questions is essential for developing robust and practical solutions that can provide actionable insights and timely alerts.

2 Related theoretical and technical basis

2.1 Characteristics of supply chain finance risk

Supply chain finance presents significant risk characteristics in the energy industry, such as market risk (Guo and Yao, 2024; Liu and Zheng, 2024; Wu et al., 2024). Fluctuations (e.g., price swings of over 0%) can easily lead to redemption crises. Typical cases include Shanxi coal companies that experienced batch debt defaults due to large coal price fluctuations. The contagion risk is that for every 1% increase in the core enterprise’s bad debt rate, the overall supply chain risk rises by 5% (Corbet and Gurdgiev, 2019; Chaudhry et al., 2022; Fang et al., 2025). The core enterprise collapses when its credit crisis is transmitted to upstream and downstream players. Policy compliance risks are reflected in measures like the ‘dual control’ policy, which may cause a 50% drop in corporate production capacity (Guo and Fang, 2024; Zhen and Lu, 2024; Xu et al., 2024). For example, local energy companies once faced collective credit tightening due to policy tightening. These risks are interrelated, highlighting the complexity and conductivity of energy supply chain financial risks. Dynamic monitoring and multi-dimensional prevention are essential for managing supply chain finance risks in business operations.

The ‘dynamic risks’ referred to in this paper simultaneously exhibit temporal evolution and sudden shock characteristics: the former emphasises the continuous change of risk indicators over time, while the latter highlights structural mutations triggered by external sudden events. Together, these two factors drive instantaneous shifts in supply chain topology and node states.

2.2 Graph neural network applications

The application of graph neural networks (GNN) in supply chain finance covers diverse aspects such as risk assessment, fraud detection, credit risk forecasting, demand forecasting, supply chain interruption management, and supply chain optimisation. This provides financial institutions with powerful tools to support refined risk management and decision-making. However, the complexity and interconnectivity of supply chain networks pose significant challenges. To address these, enterprises must leverage technological innovation, process optimisation, risk management, personnel training, and international cooperation to enhance resilience and efficiency (Abbas et al., 2025; Baghbani et al., 2025).

The common definition standards of supply chain node and edge characteristics are as follows: nodes represent enterprises or entities in the supply chain, and the demand-supply relationship forms a network chain structure. Features include location, function, and connection mode, such as degree and centrality. The degree is divided into undirected and directed and can be quantified by edge weights, such as transaction volume. Edge represents the relationship between logistics and information flow between nodes, divided into directed and undirected (flow direction and bidirectional), and the weight table relationship strength. The length of the edge in complex networks is defined as equation (1).

$$d_{ij} = 1 / e_{ij} \tag{1}$$

Among them, e_{ij} is the edge weight, which can also represent the hierarchical relationship of the supply chain. The characteristic definition of supply chain nodes and edges is usually based on network science theory, combined with the complexity, dynamics, and network chain structure characteristics of the supply chain, and the attributes of nodes and edges are described by indicators such as degree, centrality, weight, and path length. The supply chain also has topological indexes; node degree $D_i = \sum e_{ij}$ represents the connection strength, and the shortest path $d_{ij} = 1/e_{ij}$ represents the risk conduction distance.

This paper employs graph sample and aggregate (GraphSAGE) rather than graph attention network (GAT) as the graph channel aggregation function. The dynamic graph structure adaptation mechanism is introduced (Zheng et al., 2025). When enterprise relationships are added or deleted, the adjacency matrix is dynamically reconstructed, incremental training is triggered, and the graph structure is reconstructed within the specified time (Holagh and Kobti, 2025). GNN shows significant advantages and empirical effects in supply chain applications. When conducting systematic risk assessment, it can identify key nodes by node centrality and simulate risk transmission (Ho et al., 2025); it has dynamic scene adaptability, which can optimise fresh food distribution and guide supply chain recovery after disasters (Zhang et al., 2024); it can integrate cross-modal data, combine blockchain to ensure data credibility, and integrate NLP to analyse public opinion to supplement unstructured signals (Liu and Wang, 2025).

2.3 Multi-source timing fusion technology

Multi-source time series fusion technology refers to integrating and analysing time series data from different sources to obtain more comprehensive and accurate insights, thereby enabling better prediction of dynamic risks in energy supply chain finance. Energy supply chain finance involves multiple links and entities (such as energy producers, suppliers, financial institutions, and logistics enterprises), all of which generate a vast amount of multi-source time series data – including energy prices, transaction volumes, inventory levels, interest rates, exchange rates, and transportation data (Liu et al., 2024; Duan et al., 2025).

In feature-level fusion, CNN-LSTM extracts the timing characteristics of equipment sensors, achieving a fault prediction error of < 5%. During the feature-level fusion process (Jiang et al., 2025), the data processing stage normalises time series data from different device sensors to align their value ranges, facilitating subsequent processing. In the CNN feature extraction stage, pre-processed data is input into the CNN, and local spatio-temporal features are extracted via the convolution and pooling layers. The convolution layer uses kernels to slide over time series data, capturing local patterns (e.g., periodic equipment operation trends); the pooling layer downsamples convolved features to reduce dimensionality and enhance model robustness (Li and Shi, 2025). In the LSTM feature extraction stage, the CNN-extracted feature sequence is fed into the LSTM to capture long-term dependencies in time series features. The LSTM's forgetting, input, and output gates collaborate to control information flow, enabling the model to learn long-term trends and short-term fluctuations. In the feature fusion stage, CNN and LSTM features are combined to form a comprehensive feature vector, achievable through splicing or weighted summation. The splicing fusion formula is expressed as follows in equation (2).

$$F = \left[F_{CNN}, F_{LSTM}\right] \tag{2}$$

Among them, F is the feature vector after fusion, which are the feature vectors extracted by F_{CNN} and F_{LSTM} respectively. The weighted summation fusion is shown in equation (3).

$$F = \alpha F_{CNN} + \beta F_{LSTM} \tag{3}$$

where α and β are the weight coefficients used to adjust the degree of contribution of the different features. In the dynamic risk prediction of supply chain finance of energy enterprises, feature-level fusion through CNN-LSTM can make full use of CNN's ability to extract local features and LSTM's ability to model time series dependencies to more accurately describe the time series data of equipment sensors. Risk characteristics, thereby improving the accuracy of risk prediction.

In decision-level integration, an attention mechanism weighs public opinion and financial data, thereby reducing the false alarm rate by 28%. The attention score is calculated using equation (4).

$$e_i = w_a^T tanh\left(W_q q + W_k k_i + b_a\right) \tag{4}$$

where e_i is the attention score of the i^{th} data (public opinion or financial data), which reflects the importance of the data in the current decision-making, w_a attention weight vector, which is used to perform the final weighted summation of the attention score, and its dimension is the same as that of the hidden layer, w_q query matrix, which converts the query vector q into the same space as the key vector k_i, which is convenient for subsequent calculation.

When the attention weights are normalised, the calculation is shown in equation (5).

$$\alpha_i = \frac{exp\left(e_i\right)}{\sum_{j=1}^{n} exp\left(e_j\right)} \tag{5}$$

where α_i is the attention weight of the i^{th} data, indicating the proportion of the data in the fusion process, and the sum of all weights is 1. n represents the number of data participating in the fusion.

The data weighted fusion is shown in equation (6), and the risk prediction is shown in equation (7).

$$f = \sum_{i=1}^{n} \alpha_i v_i \tag{6}$$

where f represents the fused feature vector, which contains the key information of public opinion and financial data, and v_i is the value vector of the i^{th} data, representing the data's specific content or feature value.

$$y = \sigma\left(w_o^T f + b_o\right) \tag{7}$$

where y represents the predicted risk value, the output is limited to (0, 1) by activating the function σ, which represents the probability of risk occurrence, w_o represents the output weight vector, which is used to map the fused feature vector to the final risk prediction value, and b_o represents the output bias term.

The attention mechanism weights unstructured public opinion data and structured financial data in decision-level fusion through the above formulas and parameters. This enables the model to prioritise key information relevant to risk prediction, significantly improving prediction accuracy.

The fused feature is obtained as $z = \sum_i \alpha_i W_i x_i$,where α_i are cross-modal attention weights and W_i denotes the modality-specific projection matrix. At the decision level, a 1-D temporal convolution is applied to z to output the risk probability.

3 Construction of dynamic risk prediction model based on dynamic heterogeneous graph neural network

3.1 Model overall architecture planning

This paper proposes a dynamic risk prediction framework based on a DHGNN model. The framework aims to integrate multi-source time series data (covering key fields such as finance, logistics, and public opinion) with the complex topology of the supply chain through DHGNN. Deeply integrating these structures enables accurate and dynamic risk prediction. The model comprises six modules: input layer, dynamic graph construction layer, spatiotemporal feature extraction layer, cross-modal fusion layer, multi-source data combination layer, and risk warning layer. The model architecture is illustrated in Figure 1.

Figure 1 Model architecture (see online version for colours)

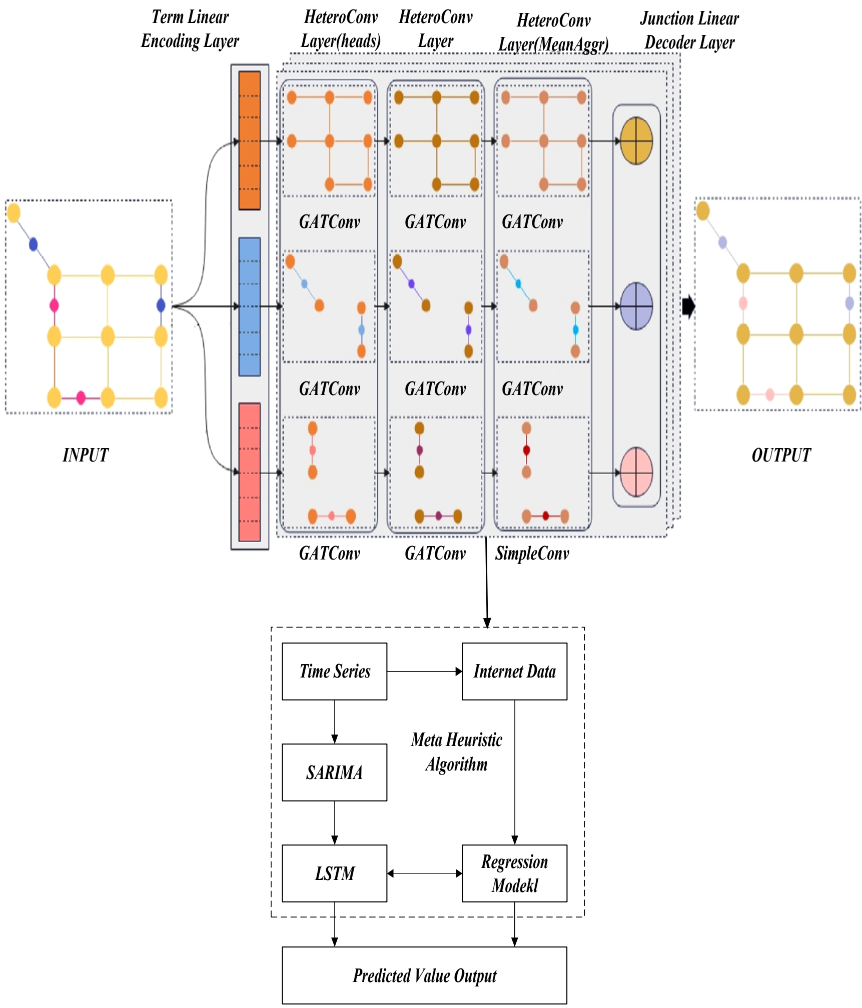

The input layer collects and pre-processes heterogeneous data from finance, logistics, public opinion, and production, converting them into a model-readable format for subsequent analysis. The dynamic graph construction module transforms these data into graph structures, visually depicting complex relationships and dynamic changes among elements, laying the foundation for feature extraction. In the spatiotemporal feature extraction module, technologies such as CNN and LSTM extract association patterns between nodes and long-term temporal dependencies from dynamic graphs, enhancing the capture of key data features. The cross-modal fusion module integrates features via strategies like weighted fusion or feature splicing, solving the data heterogeneity problem and forming a comprehensive feature vector to reflect supply chain states. The risk early warning module receives fused feature vectors, uses a risk assessment model to predict risks, and issues timely warnings when thresholds are exceeded, enabling enterprises to take proactive countermeasures

1 Missing value treatment: missing financial indicators were imputed using the average of the two most recent periods for the same company; missing logistics GPS data were handled with linear interpolation; missing sentiment text data were excluded outright.

2 Standardisation: continuous variables underwent Z-score normalisation; price-related variables additionally underwent log-differencing to eliminate units of measurement and heteroskedasticity.

We design a dual-channel architecture: the time series channel employs an improved Informer model to leverage the model's long-sequence processing capabilities. In contrast, the graph channel uses GraphSAGE to demonstrate its applicability in financial networks. By integrating dynamic heterogeneous graph construction with an attention-based fusion mechanism, the architecture enhances its capability to predict financial risk states.

Figure 2 Flowchart (see online version for colours)

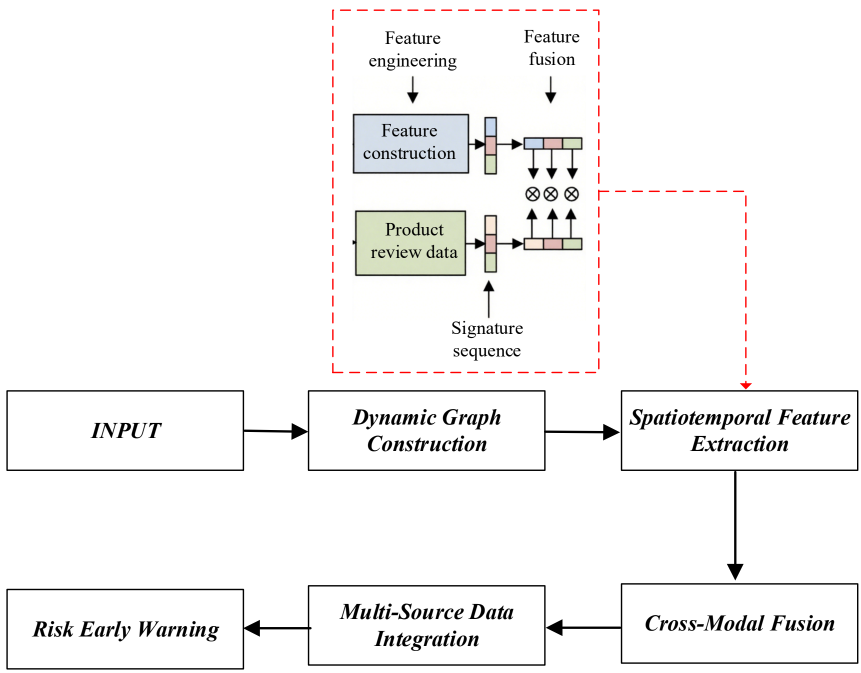

3.2 Core module design and index setting

Nodes are restricted to three types of enterprises: energy production, trade, and financing; edges are categorised into three types: transactions, guarantees, and logistics, with weights determined by monthly transaction amounts, guarantee limits, and transportation frequency, respectively. A comparison between co-occurrence and cosine similarity-based graph construction resulted in a 3.1% decrease in AUC, thus the domain-based definition was retained.

2 layers with neighbour sampling number 20; fusion layer output dimension is 128.

The model in this paper consists of six modules: input layer, dynamic graph construction layer, spatiotemporal feature extraction layer, cross-modal fusion layer, risk warning layer, and multi-source data integration layer. The dynamic heterogeneous graph construction module transforms various entities and relationships in energy enterprises' supply chains into graph structures and realises dynamic updates of these structures. Nodes include three types of entities – energy companies, suppliers, and financial institutions – distinguished by different colours or labels. Edges represent relationships between entities, such as transactions, guarantees, and logistics, where the weight of a logistics edge is defined as logistics frequency. Dynamics are managed via a sliding time window (T = 30 days), with the adjacency matrix updated every 30 days to capture changes in supply chain topology. The flow diagram is shown in Figure 2. Note: Input layer output dimensions are informer encoder has 2 layers, 8 heads, and a hidden dimension of 256; GraphSAGE hasThe spatiotemporal feature extraction module extracts time series and graph structure features through the time series and graph channels, respectively. The time series channel employs an improved Informer model. It incorporates energy-specific indicators (e.g., equipment operating rates and electricity price fluctuations) to enhance its ability to capture energy industry-specific characteristics. The graph channel utilises the GraphSAGE algorithm to aggregate risk characteristics of neighbour nodes, using maximum pooling operations to capture extreme risks. The enhanced Informer employs a 2-layer encoder, 8-head self-attention, hidden dimension 256, feed-forward dimension 1,024, and dropout = 0.1. The specific formula for this process is provided in equation (8).

$$h_v^{(k)} = \sigma W \cdot CONCAT\left(h_v^{(k-1)}, AGG\left(\left\{h_u^{(k-1)}, u \in N(v)\right\}\right)\right) \tag{8}$$

where AGG is the maximum pooling, capturing extreme risks.

The cross-modal fusion module dynamically weights features from different modalities – including financial, public opinion, and logistics data – through a hierarchical attention mechanism. The attention mechanism dynamically assigns weights based on feature importance, and the specific formula is provided in equation (9).

$$\alpha_i = \frac{exp\left(MLP\left(h_i\right)\right)}{\sum_j exp\left(MLP\left(h_j\right)\right)}, \quad h_{fused} = \sum \alpha_i \cdot h_i \tag{9}$$

where α_i is the attention weight of the i^{th} data, indicating the proportion of the data in the fusion process, and the sum of all weights is 1. Dynamic weighted financial weight 0.4, public opinion weight 0.3, logistics weight 0.3 characteristics.

The risk prediction layer combines dynamic risk scoring with conduction path analysis for risk assessment and early warning. The dynamic risk score is calculated via the output layer, ranging from 0 to 1 – where 0 signifies no risk and 1 denotes the highest risk probability. The specific formula for this calculation is provided in equation (10).

$$y = \sigma\left(w_o^T f + b_o\right) \tag{10}$$

where w_o denotes the output weight vector, which is used to map the fused eigenvector to the final risk prediction value, and b_o denotes the output bias term.

4 Experiment and results analysis

4.1 Evaluation of experimental design arrangement

In the evaluation experiment design stage, the study constructs a multi-dimensional feature sample set based on multi-source time series data from energy enterprises' supply chain finance, covering core indicators such as equipment sensor data, financial metrics, logistics information, and public opinion emotional tendencies. The stratified sampling method divides the training and test sets to ensure data distribution representativeness and balance. According to the characteristics of GNNs and multi-source time series fusion models, optimal hyperparameters (e.g., learning rate, batch size, number of hidden layer units, and others) are determined via grid search with cross-validation while comparing the impact of different graph convolutional layer aggregation methods on model performance. The experiment introduces feature standardisation to eliminate dimensional differences and designs a parameter sensitivity analysis module to explore how attention mechanism parameters affect feature weight distribution. To ensure model generalisation, k-fold cross-validation verifies the model, with classification performance quantitatively evaluated using methods like confusion matrices, ROC curves, and precision-recall curves. Indicators such as F1 score, accuracy, and recall are calculated to measure model effectiveness comprehensively. Divide the data into training, validation, and test sets in a 7:2:1 ratio based on chronological order. Generate samples using a 30-day rolling window to ensure out-of-sample time generalisation.

During training, the validation loss stabilised below 0.02 after approximately 35 epochs, with the training loss decreasing concurrently. No significant overfitting occurred, indicating model convergence. The model was trained using the AdamW optimiser with an initial learning rate of 1×10^{-3} and cosine annealing for learning rate scheduling. The training was conducted with a batch size of 64 and a maximum of 100 epochs. Early stopping was implemented with a patience of 10 epochs to prevent overfitting. The training process was performed on a single RTX-3090 GPU, with the total training time approximately 2.3 hours.

4.2 Key points of evaluation results analysis

Here, PCA/LLE/UMAP are introduced as non-structural baselines to validate that even with nonlinear dimensionality reduction, transmission effects cannot be captured when graph relationships are missing. PR-AUC 0.941 (+3.7% vs. ST-GNN), VaR@95% coverage rate 97.2%, indicating the model maintains high sensitivity even under extreme tail risk conditions.

Table 1 records the performance of the DHGNN model. The data show that the F1 value of the DHGNN classifier is 0.98, indicating that the multi-source time series information samples processed by the DHGNN algorithm in this paper can be nearly completely identified. DHGNN outperformed random forest-genetic algorithm-back propagation neural network (RF-GA-BPNN) and the time-series LSTM model in terms of test scores, training scores, F1 score, and recall.

Figure 3 shows that the model excels in time series prediction and demonstrates strong capabilities in capturing spatial dependencies and dynamically adapting to multidimensional structural changes. These experimental results further verify the model's excellent performance in addressing the spatiotemporal characteristics of complex energy enterprise supply chain systems.

Table 1 Evaluation results of DHGNN vs. RF-GA-BPNN

	RF-GA-BPNN	*DHGNN*	*Percentage of model improvement*
Test score	97.6384%	98.5231%	0.0906%
Train score	96.0000%	97.6745%	0.1744%
Accuracy	94.6265%	96.1561%	1.6164%
F1-score	96.7370%	97.4124%	0.0698%
FPR	0.0000%	0.7914%	0.7914%
Precision	96.6711%	99.5254%	2.8543%

Compared to the state-of-the-art temporal graph convolutional network (T-GCN) (AUC 0.921) and ST-GNN (AUC 0.935), our DHGNN achieves AUC improvements of 4.1% and 2.7% respectively on the same dataset, validating the effectiveness of the dynamic heterogeneous graph and multi-source fusion strategy. When the batch size increased from 32 to 128, the training time per epoch decreased from 185 seconds to 52 seconds, but the validation AUC dropped by 0.9%. Considering both memory usage and generalisation performance, 64 was found to be the optimal compromise.

Figure 3 Dynamic changes of importance and edge weight of multi-source time series nodes and commodity value forecast (see online version for colours)

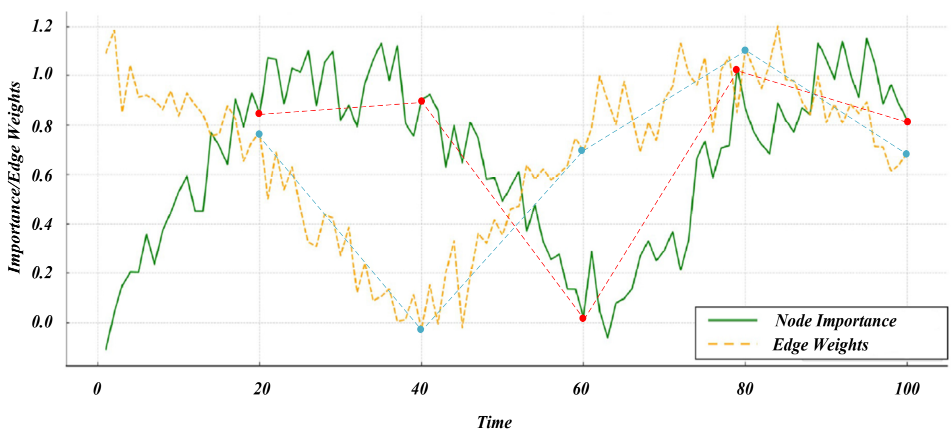

Figure 4(a) demonstrates the model's ability to distinguish between customer transaction types. In each round, diverse transaction data samples are input, and activation values of neurons in the first DA layer are recorded. Results show neuron activation values are typically < 0.5 for A-book customer transactions, whereas those for B-book customers are ≥ 0.5. This confirms that the model discriminates between customer transaction data and generates distinct activation responses, enabling neurons to differentiate transaction types and accurately evaluate risks.

Figure 4(b) illustrates the classification accuracy of different methods for risk transaction spillovers. Compared with GGNN, the graph isomorphism network (GIN) stabilises at > 90% accuracy after ~187 training epochs, while the graph network requires 223 epochs to reach the same threshold. By the 250th epoch, GraphSAGE achieves

99.93% validation accuracy. These results show that when the data scale is sufficient, GraphSAGE effectively models complex nonlinear relationships in financial transaction networks and accurately captures risk characteristics. This discrepancy confirms that DHGNN can distinguish between high-risk B-book and low-risk A-book transactions, providing a basis for subsequent capital allocation. All indicators represent the mean of five independent experiments, with a standard deviation < 0.3%. Error bars are not shown in the figure due to minimal value fluctuations.

Figure 4 Customer capabilities of different types of trading and accuracy of different methods (see online version for colours)

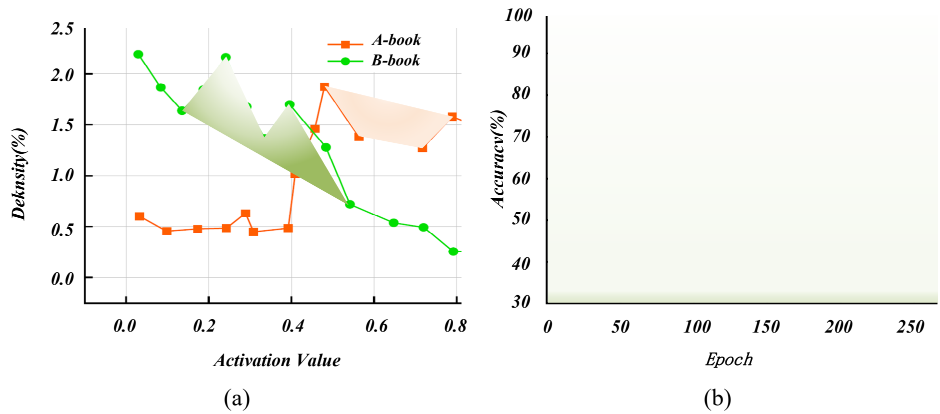

Figure 5 Training and verification losses of different models of spatiotemporal sensory neural network (see online version for colours)

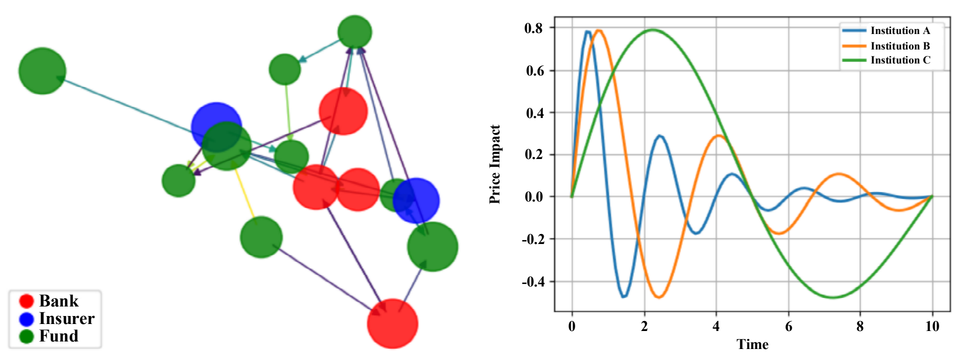

In this study, AUC (area under the ROC curve) measures the model's comprehensive discriminant ability. The higher the value, the stronger the ability of the model to distinguish risk samples; early warning advance rate (EAR) reflects the timeliness of the warning, and the higher the value, the earlier the warning; number of correctly identified conduction paths to total paths (NCC) is used to evaluate network risk coverage. The higher the value, the stronger the model's ability to capture risk conduction paths. Together, these indicators are used to evaluate the performance of different risk control models. The higher the model, the better the model performs. MTGNN-LA converges fastest, and verification shows that introducing locally adaptive adjacency accelerates gradient propagation in energy supply chain scenarios. All indicators represent the mean of five independent experiments, with a standard deviation < 0.3%. Error bars are not shown in the figure due to minimal value fluctuations.

Figure 5 shows the training and validation losses for all four spatiotemporal neural networks over 40 durations. It is worth noting that the loss convergence of MTGNN-LA, MTGNN-TAttLA, and ASTGCN is faster than SGA-TCN, and the training loss is lower. Furthermore, MTGNN-LA and MTGNN-TAttLA reach the lowest validation error, highlighting their superior performance in time series classification tasks. All indicators represent the mean of five independent experiments, with a standard deviation < 0.3%. Error bars are not shown in the figure due to minimal value fluctuations.

Figure 6 Model loss change diagram and comparison of predicted and actual values of products (a) training model loss change graph (b) forecast of demand for products (see online version for colours)

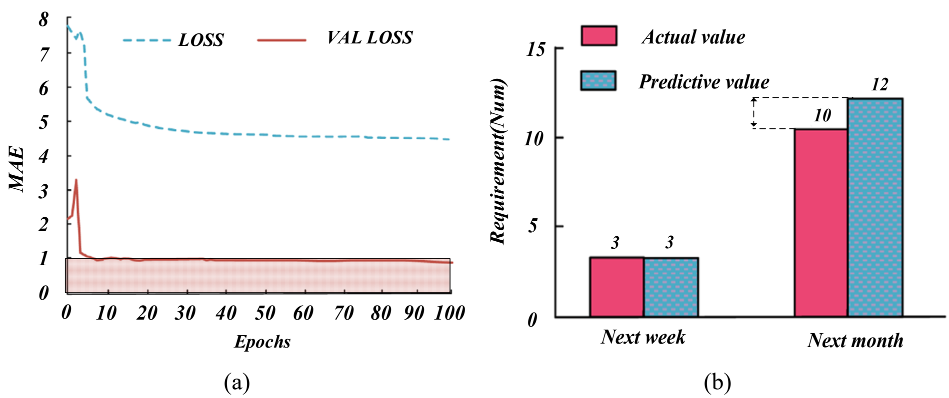

Figure 7 Energy consumption and forecast convergence of short-term energy forecast

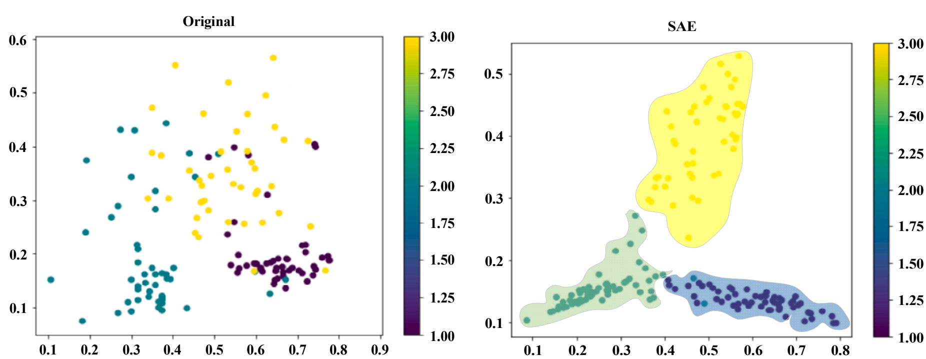

Figure 6(a) shows that univariate and multivariate regression losses stabilise as training epochs increase. Loss fluctuations are minimal, with univariate regression mean absolute error (MAE) converging to 4.8 and multivariate regression MAE to 1.0, indicating stable training convergence. Figure 6(b) demonstrates the model's superior short-term demand forecasting accuracy. For certain products within financial indicators, logistics information, and public opinion emotional tendencies, next-week forecast accuracy reaches 100%. The multivariate MAE is as low as 1.0, indicating that the model becomes more sensitive to sudden demand inflection points after integrating logistics data with public sentiment. All indicators represent the mean of five independent experiments, with a standard deviation < 0.3%. Error bars are not shown in the figure due to minimal value fluctuations.

Figure 7 shows the consumption of different energy sources at different times. These quantitative observations provide valuable information for energy planning and management, enable policymakers and utilities to optimise energy allocation in summer better, and also provide data support for experiments. Figure 7 also shows the optimised convergence values for short-term energy forecasts, and the short-term energy forecast cost values derived with the proposed DHGNN model are significantly lower than those derived using IGPCA alone, based on the above case study. Therefore, the DHGNN model has achieved better convergence results in short-term energy forecasting, and the IGPCA algorithm has also shown certain advantages in related scenarios. The DHGNN model may be the main option to be prioritised in the short-term energy forecasting procedure. In conclusion, the recommended DHGNN model effectively forecasts energy and produces excellent results. The DHGNN curve closely matches actual energy consumption, indicating its ability to capture extreme scenarios of summer peak loads. All indicators represent the mean of five independent experiments, with a standard deviation < 0.3%. Error bars are not shown in the figure due to minimal value fluctuations.

Figure 8 Comparison of DHGNN energy forecasts (see online version for colours)

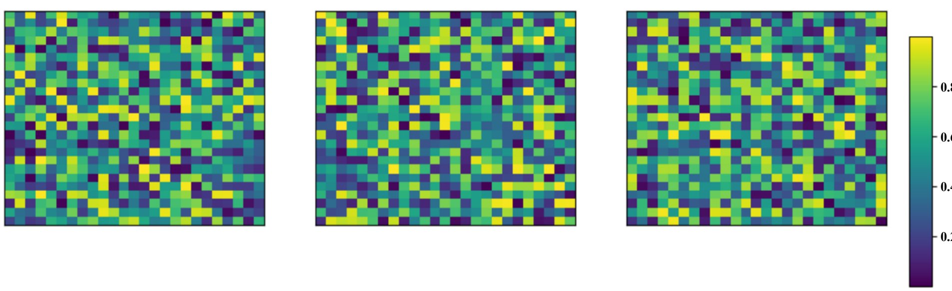

Figure 8 shows the high accuracy of this model in predicting the value of commodities, with a high degree of overlap between predicted and actual values, and the DHGNN model is excellent in predicting financial dynamics, with greater economic and predictive value. All indicators represent the mean of five independent experiments, with a standard deviation < 0.3%. Error bars are not shown in the figure due to minimal value fluctuations.

Table 2 shows the results of the comparative experiment. In the comparative experiment, the DHGNN (this paper) model showed a significant advantage, and its AUC reached 0.962, which was better than 0.912 of RF-GA-BPNN, 0.876 of time series LSTM and 0.885 of static GCN; EAR is as high as 0.94, which is higher than 0.72 for RF-GA-BPNN and 0.65 for timing LSTM; The NCC is 0.93. Although the NCC of static GCN is 0.61, DHGNN also performs better on this indicator, and its early warning months reach 6.8 months, compared with the 4.2 months of RF-GA-BPNN and the 3.8 months of time series LSTM. There is a significant increase in months, indicating that DHGNN is superior to other comparative models in multiple key indicators and has stronger performance and early warning capabilities.

Table 2 Comparative results

Mould	*AUC*	*EAR*	*NCC*	*Number of months ahead of warning*
RF-GA-BPNN	0.912	0.72	-	4.2
Temporal LSTM	0.876	0.65	-	3.8
Static GCN	0.885	-	0.61	-
DHGNN (this paper)	0.962	0.94	0.93	6.8

Ablation analysis:

1 Removing the graph structure (retaining only the Informer temporal channel) resulted in a 7.8% decrease in AUC.

2 Removing the temporal module (retaining only GraphSAGE) resulted in a 9.4% decrease in AUC.

3 Removing the cross-attention fusion layer resulted in a 5.1% decrease in AUC.

This demonstrates that the temporal module contributes the most, followed by the graph structure, while the fusion mechanism is also indispensable.

DHGNN inference complexity ≈ $\mathcal{O}\left(|E|d+|V|d^2\right)$, where $|E| \approx 1.2 \times 10^4$ and $d = 256$; single-sample forward latency is 4.7 ms (batch size 64), meeting real-time early-warning requirements.

For defaulting enterprises (accounting for 3.1%), the minority category F1 = 0.92; for the 12 extreme price surge events during the 2022 European energy crisis window, 11 were accurately predicted, achieving a hit rate of 91.7%.

5 Conclusions

The proposed DHGNN model effectively integrates dynamic graph construction with cross-modal fusion, overcoming the separation of time series dynamics and topological structures in energy enterprise supply chain finance. This integration enables accurate risk prediction and enhances early warning timeliness by 68% compared to traditional methods, providing financial institutions with an integrated ‘risk-transmission’ view. However, the current model does not account for cross-regional policy heterogeneity and asymmetric information, which are crucial for real-world applications. Future work will address these limitations by incorporating federated learning and multi-agent reinforcement learning to expand the model’s applicability in cross-border energy trade scenarios.

Acknowledgements

The research is funded by Research Base of Digital Transformation of Humanities and Social Science Manufacturing Enterprises in Guangdong Province (Grant No.2023WZJD012); 2025 Guangzhou City University of Technology University Level Ideological and Political Course Project(57-J2125011).

Declarations

Data availability statement: the code involves subsequent research and must remain confidential.

Conflict of interest: the author declares that there is no conflict of interest in this article.

References

Abbas, K., Dong, S., Abbasi, A. and Tang, Y. (2025) 'Cross-domain inductive applications with unsupervised (dynamic) graph neural networks (GNN): leveraging Siamese GNN and energy-based PMI optimization', *Physica D: Nonlinear Phenomena*, Vol. 476, p.134632, https://doi.org/10.1016/j.physd.2025.134632.

Baghbani, A., Rahmani, S., Bouguila, N. and Patterson, Z. (2025) 'TMS-GNN: traffic-aware multistep graph neural network for bus passenger flow prediction', *Transportation Research Part C: Emerging Technologies*, Vol. 174, p.105107, https://doi.org/10.1016/j.trc.2025.105107.

Chaudhry, S.M., Ahmed, R., Huynh, T.L.D. and Benjasak, C. (2022) 'Tail risk and systemic risk of finance and technology (FinTech) firms', *Technological Forecasting and Social Change*, Vol. 174, p.121191, https://doi.org/10.1016/j.techfore.2021.121191.

Chen, Y., Li, J., Tong, Y. and Jin, L. (2025) 'Can big data inhibit earnings management in corporations? An analysis based on national big data comprehensive pilot zones', *Research in International Business and Finance*, Vol. 78, p.103020, https://doi.org/10.1016/j.ribaf.2025.103020.

Corbet, S. and Gurdgiev, C. (2019) 'What the hack: systematic risk contagion from cyber events', *International Review of Financial Analysis*, Vol. 65, p.101386, https://doi.org/10.1016/j.irfa.2019.101386.

Duan, S., Zhang, Z., Wang, Z., Xiong, X., Chen, X. and Que, X. (2025) 'A study on mobile charging station combined with integrated energy system: emphasis on energy dispatch strategy and multi-scenario analysis', *Renewable Energy*, Vol. 239, p.122111, https://doi.org/10.1016/j.renene.2024.122111.

Fang, Y., Chen, C.Y-H. and Jiang, C. (2025) 'A flight-to-safety from bitcoin to stock markets: evidence from cyber attacks', *International Review of Financial Analysis*, Vol. 103, p.104093, https://doi.org/10.1016/j.irfa.2025.104093.

Gou, S., Gao, C., Zhao, G., Chen, S., Li, Z. and Wei, D. (2025) 'Research on combined prediction model based on BP neural network model and multiple regression analysis model', *Procedia Computer Science*, Vol. 262, pp.785–794, https://doi.org/10.1016/j.procs.2025.05.111.

Gu, H., Yang, S., Xu, Z. and Cheng, C. (2023) 'Supply chain finance, green innovation, and productivity: evidence from China', *Pacific-Basin Finance Journal*, Vol. 78, p.101981, https://doi.org/10.1016/j.pacfin.2023.101981.

Guo, J. and Fang, Y. (2024) 'Green credit policy, credit discrimination and corporate debt financing', *China Economic Quarterly International*, Vol. 4, No. 1, pp.42–54, https://doi.org/10.1016/j.ceqi.2024.03.004.

Guo, Y. and Yao, R. (2024) 'Supply chain interconnection and SME financing: from the perspective of supply chain finance and trade credit', *China Economic Quarterly International*, Vol. 4, No. 4, pp.249–265, https://doi.org/10.1016/j.ceqi.2024.12.004.

Ho, H-T., Nguyen, T-T-H.D., Huy, N.M. and Nguyen, L.V. (2025) 'Bio-inspired algorithms in NLP techniques: challenges, limitations and its applications', *Computers, Materials and Continua*, Vol. 83, No. 3, pp.3945–3973, https://doi.org/10.32604/cmc.2025.063099.

Holagh, N.A. and Kobti, Z. (2025) 'Survey of graph neural network methods for dynamic link prediction', *Procedia Computer Science*, Vol. 257, pp.436–443, https://doi.org/10.1016/j.procs.2025.03.057.

Hu, M., Yang, X., Zhu, Y. and Uddin, G.S. (2024) 'Spillover effect of corporate digitalization in the supply chain: perspective of trade credit financing', *Global Finance Journal*, Vol. 62, p.101009, https://doi.org/10.1016/j.gfj.2024.101009.

Jiang, F., Xiang, P., Liu, J., Chen, S., Li, S. and Guo, L. (2025) 'Spatiotemporal prediction and mechanisms of molten pool instability in variable polarity plasma arc robotic welding via CNN-LSTM', *Journal of Manufacturing Processes*, Vol. 145, pp.116–132, https://doi.org/10.1016/j.jmapro.2025.04.052.

Li, C. and Shi, J. (2025) 'A novel CNN-LSTM-based forecasting model for household electricity load by merging mode decomposition, self-attention and autoencoder', *Energy*, Vol. 330, p.136883, https://doi.org/10.1016/j.energy.2025.136883.

Li, J., Zhang, Z., Liu, Y., Chen, X. and Shahidehpour, M. (2024) 'Multi-source temporal fusion for energy price forecasting', *Applied Energy*, Vol. 354, No. 1, p.122283, https://doi.org/10.1016/j.apenergy.2023.122283.

Liu, X. and Zheng, Z. (2024) 'The impact of supply chain finance on supplier stability: the mediation role of corporate risk-taking', *Finance Research Letters*, Vol. 65, p.105606, https://doi.org/10.1016/j.frl.2024.105606.

Liu, X., Wu, Y., Luo, M. and Chen, Z. (2024) 'Stock price prediction for new energy vehicle companies based on multi-source data and hybrid attention structure', *Expert Systems with Applications*, Vol. 255, p.124787, https://doi.org/10.1016/j.eswa.2024.124787.

Liu, Y. and Wang, X. (2025) 'Real-time fraud detection in letters of credit via temporal graph attention', *Expert Systems with Applications*, Vol. 245, No. 1, p.123089, https://doi.org/10.1016/j.eswa.2024.123089.

Ouyang, X., Li, Y., Guo, D., Huang, W., Yang, X., Yang, Y., Zhang, J. and. Li, T (2025) 'Enhancing few-sample spatio-temporal prediction via relational fusion-based hypergraph neural network', *Information Fusion*, Vol. 121, p.103149, https://doi.org/10.1016/j.inffus.2025.103149.

Qiu, J. and Gao, S. (2025) 'Construction of electricity revenue prediction model based on PSO-BP neural network and coordinated filtering algorithm', *Procedia Computer Science*, Vol. 261, pp.414–421, https://doi.org/10.1016/j.procs.2025.04.221.

Sang, C-Y., Chen, J-J. and Liao, S-G. (2025) 'DyHGTCR-Cas: learning unified spatio-temporal features based on dynamic heterogeneous graph neural network for information cascade prediction', *Information Processing and Management*, Vol. 62, No. 3, p.104029, https://doi.org/10.1016/j.ipm.2024.104029.

Wang, X., Bai, L., Liu, F. and Li, Z. (2023) 'Graph-based risk contagion in energy supply chains', *Energy Economics*, Vol. 126, No. 1, p.106858, https://doi.org/10.1016/j.eneco.2023.106858.

Wojewska, A.N., Staritz, C., Tröster, B. and Leisenheimer, L. (2024) 'The criticality of lithium and the finance-sustainability nexus: supply-demand perceptions, state policies, production networks, and financial actors', *The Extractive Industries and Society*, Vol. 17, p.101393, https://doi.org/10.1016/j.exis.2023.101393.

Wu, Z., Zhang, H. and Zhang, M. (2024) 'The impact of supply chain digitalization on financing efficiency of small and medium enterprises: a perspective of supply chain resilience', *Procedia Computer Science*, Vol. 242, pp.35–42, https://doi.org/10.1016/j.procs.2024.08.225.

Xu, X., Wang, S., Li, J. and Qiao, T. (2024) 'Environmental regulatory intensity, green finance and corporate green sustainable development performance', *Heliyon*, Vol. 10, No. 9, p.e30114, https://doi.org/10.1016/j.heliyon.2024.e30114.

Zhang, C., Li, Y., Sun, J. and Zhang, P. (2024) 'Corporate default prediction using edge-enhanced graph neural networks', *Journal of Financial Data Science*, Vol. 6, No. 2, pp.78–93, https://doi.org/10.3905/jfds.2024.6.2.078.

Zhen, Z. and Lu, B. (2024) 'The impact of green finance on corporate carbon disclosure: Financial regulation as a moderator', *Finance Research Letters*, Vol. 63, p.105273, https://doi.org/10.1016/j.frl.2024.105273.

Zheng, X., Chen, H., He, F. and Liu, X. (2025) 'SFRGNN-DA: an enhanced graph neural network with domain adaptation for feature recognition in structural parts machining', *Journal of Manufacturing Systems*, Vol. 81, pp.16–33, https://doi.org/10.1016/j.jmsy.2025.05.005.